

# TruckV2X: A Truck-Centered Perception Dataset

Tenghui Xie<sup>1</sup>, Zhiying Song<sup>1</sup>, Fuxi Wen<sup>1</sup>, *Senior Member, IEEE*, Jun Li<sup>1</sup>, Guangzhao Liu<sup>2</sup> and Zijian Zhao<sup>2</sup>

**Abstract**—Autonomous trucking offers significant benefits, such as improved safety and reduced costs, but faces unique perception challenges due to trucks’ large size and dynamic trailer movements. These challenges include extensive blind spots and occlusions that hinder the truck’s perception and the capabilities of other road users. To address these limitations, cooperative perception emerges as a promising solution. However, existing datasets predominantly feature light vehicle interactions or lack multi-agent configurations for heavy-duty vehicle scenarios. To bridge this gap, we introduce TruckV2X, the first large-scale truck-centered cooperative perception dataset featuring multi-modal sensing (LiDAR and cameras) and multi-agent cooperation (tractors, trailers, CAVs, and RSUs). We further investigate how trucks influence collaborative perception needs, establishing performance benchmarks while suggesting research priorities for heavy vehicle perception. The dataset provides a foundation for developing cooperative perception systems with enhanced occlusion handling capabilities, and accelerates the deployment of multi-agent autonomous trucking systems. The TruckV2X dataset is available at <https://huggingface.co/datasets/XieTenghui1/TruckV2X>.

**Index Terms**—Vehicle-to-everything, Cooperative Perception, Autonomous Trucking, Dataset.

## I. INTRODUCTION

**A**UTONOMOUS trucking is expected to benefit the logistics industry in improved road safety, reduced operational costs, and solutions to driver shortages [1]. As an indispensable yet high-impact participant in modern transportation systems, the safe deployment of intelligent trucks hinges on two critical factors: their ability to comprehensively perceive their surroundings and to operate without impairing the safety or perceptual abilities of other road users.

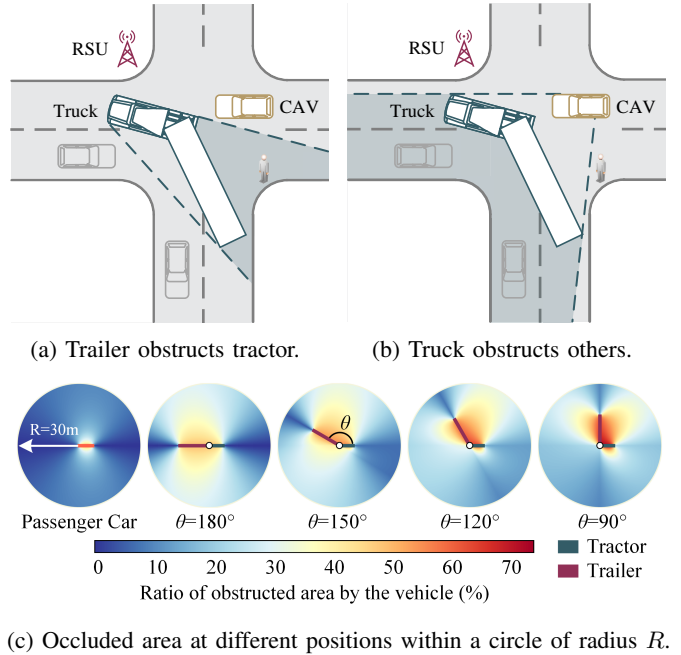
These factors emerge from the operational constraints of tractor-trailer systems. Their substantial dimensions create persistent blind zones (Figure 1a, 1b), where structural components obstruct both self-perception and neighboring agents’ sensing capabilities. Articulated motion further exacerbates occlusions through dynamic spatial conflicts between tractors and trailers during maneuvers [2]. Compounding these issues, low-speed operation combined with large spatial footprints induces sustained environmental uncertainties in mixed traffic, systematically expanding risk zones [3].

Manuscript received: March 18, 2025; Revised: May 23, 2025; Accepted: July 11, 2025. This paper was recommended for publication by Editor Hyungil Moon upon evaluation of the Associate Editor and Reviewers’ comments. (*Corresponding author: Fuxi Wen*)

<sup>1</sup>Tenghui Xie, Zhiying Song, Fuxi Wen, and Jun Li are with the School of Vehicle and Mobility, Tsinghua University, Beijing 100190, China (e-mail: wenfuxi@tsinghua.edu.cn).

<sup>2</sup>Guangzhao Liu and Zijian Zhao are with FAW Jiefang Group Co., Ltd., Changchun 130011, China.

Digital Object Identifier (DOI): see top of this page.



(c) Occluded area at different positions within a circle of radius  $R$ .

Fig. 1: Illustration of truck-related occlusions.

As an example, Figure 1c illustrates how visibility is obstructed within a 30-meter observational range. While standard passenger cars retain a relatively clear view (<30% occlusion area), tractor-trailers display 1.5× greater baseline occlusion even when driving straight. The problem intensifies as trailers pivot: angular displacement between tractor and trailer steeply degrades visibility, with occlusion surpassing 70% during 90° turns. These dual challenges, sheer vehicle size, and pivoting motion patterns, collectively position articulated trucks as high-risk urban blind zone generators.

Numerous efforts have been made in human-driven trucks to design blind-spot detection systems [4], [5]. There are two potential directions to further enhance the perception intelligence of trucks. First, advanced data-driven algorithms are needed to achieve comprehensive perception by integrating information from the tractor and trailer. Second, cooperative perception systems can enable trucks to share data with other road users and infrastructures. By leveraging Vehicle-to-Everything (V2X) communication technology, we can connect the tractor and trailer internally, allowing them to perceive the environment collaboratively. Additionally, trucks can communicate with external agents, such as connected and automated vehicles (CAVs) and roadside units (RSUs), enabling seamless sensor data integration from diverse sources. This integration of multi-perspective information broadens the perceptual range of all agents and helps overcome occlusions, enhancing overall

traffic safety and efficiency.

However, the development of such systems is significantly impeded by a lack of suitable datasets. As highlighted in Figure 2, existing datasets, such as nuScenes [6] and Waymo Open Dataset [7], are primarily designed for light vehicles and fail to account for the unique challenges of trucks. Similarly, cooperative perception datasets like OPV2V [8] and DAIR-V2X [9] focus on light vehicles, while truck-specific datasets such as Man TruckScenes [10] are limited to single-agent setups with sensors mounted only on the tractor, ignoring the critical role of trailers and the need for cooperative perception.

To bridge these gaps, we present TruckV2X, the first truck-centered perception dataset, featuring multi-modal sensing (LiDAR and cameras) and multi-agent cooperation (tractors, trailers, CAVs, and RSUs). Utilizing Unreal Engine, we modeled a semi-trailer truck and integrated it into the CARLA simulation environment [11] as an interactive agent. The truck has two 64-channel LiDARs and five surround-view cameras on both the tractor and the trailer. Other agents, including one CAV and one RSU, are also equipped with LiDARs and multi-view cameras. The dataset comprises 64 scenarios, featuring 88,396 frames of LiDAR point clouds, one million camera images, and 1.18 million 3D bounding box annotations. Each object is annotated with a bounding box, ID, speed, and other relevant information, supporting tasks such as object detection and tracking. Additionally, we provide eight benchmark implementations for cooperative perception tasks and conduct extensive experimental analysis on occlusion scenarios, demonstrating the critical value of truck-specific viewpoints for cooperative perception.

Overall, the main contributions of this work include:

- We propose TruckV2X, the first truck-centered multi-modal and multi-agent cooperative perception dataset, addressing data scarcity for truck-specific challenges such as trailer occlusions and multi-agent cooperation.
- We provide a benchmark for truck-centered collaborative perception to encourage further research and advance cooperative technologies for truck perception safety.
- Through quantitative analysis, we propose the concept of trucks as mobile perception platforms, demonstrating their dual role as both occlusion sources and enhancers in reducing environmental occlusions.

## II. RELATED WORK

*Perception of truck:* Previous studies have developed perception-assisted systems in human-driven trucks to reduce blind spots and enhance state estimation capabilities. These systems often rely on additional sensors, such as millimeter-wave radar and cameras, to improve driver awareness and safety [4], [5]. Recent advancements have also explored the integration of computer vision for more robust perception and state estimation [12]. In terms of datasets, despite progress in autonomous driving perception, most datasets focus on light vehicles, leaving a significant gap. TuSimple [13] includes some heavy vehicle data but is limited in scope and volume. MAN TruckScenes [10], the first large-scale multi-modal dataset for heavy vehicles, lacks comprehensive trailer-mounted sensor data and multi-agent setups. In this work,

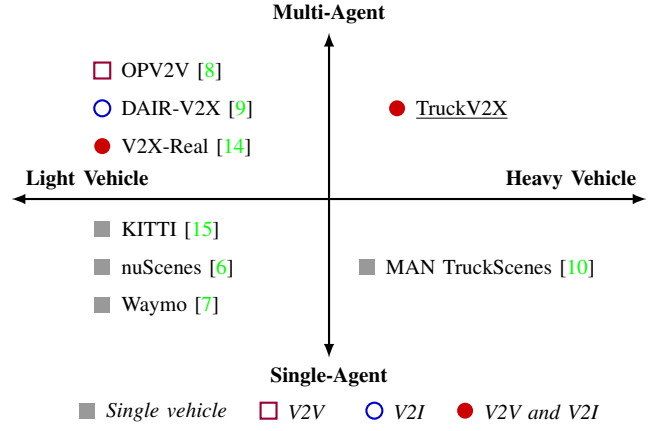


Fig. 2: Datasets available for the perception of autonomous driving. TruckV2X is the first multi-agent collaborative perception dataset specifically designed for heavy vehicles. (V2V: Vehicle-to-Vehicle, V2I: Vehicle-to-Infrastructure)

TruckV2X provides multi-modal data from the tractors, trailers, CAVs, and RSUs, offering a foundation for blind spot detection, state estimation, and environmental perception in heavy vehicles.

*V2X perception and datasets:* V2X technology has been applied in heavy vehicles for tasks such as collision warning [16] and platooning [17]. While V2X systems primarily transmit basic information, no studies have proposed datasets for high-level cooperative perception that include trucks as cooperative agents [18]. On the other hand, recent years have seen significant progress in cooperative perception datasets for passenger cars: OPV2V [8] pioneered synthesized multi-vehicle perception data, while DAIR-V2X [9] marked the first real-world V2I dataset for object detection. Numerous other datasets have since been introduced [19], [14], [20]. They focus on light vehicles, leaving a critical gap for heavy vehicles. In cooperative perception, heavy vehicles present unique challenges, such as significant occlusions caused by the large size and dynamic movements of tractors and trailers. These occlusions not only hinder the truck's perception but also disrupt other agents in the cooperative system. The proposed dataset, TruckV2X, bridges these gaps by generating large-scale occlusion scenarios and providing multi-view data from tractors, trailers, CAVs, and RSUs, offering a foundation for advancing cooperative perception in heavy vehicles.

## III. DATASET

### A. Vehicle configurations

TruckV2X is the first to incorporate semi-trailer trucks into autonomous driving simulation environments for cooperative perception applications. Focusing on urban-prevalent container trucks (tractor-trailer combinations), we developed high-fidelity models through a sequential workflow. First, using Blender, we constructed and optimized articulated vehicle skeletons with reduced mesh complexity. These models were then imported into Unreal Engine, where the tractor and trailer were linked via physics-based kinematic constraints within the

TABLE I: Key parameters of the truck in our dataset.

	Weight (kg)	Length (m)	Width (m)	Height (m)	CG Height (m)
Tractor	8,805	6.51	3.05	4.20	2.18
Trailer	20,000	14.25	2.71	4.40	2.06

TABLE II: Sensor specifications for each agent.

Agents	Sensors	Details
Tractor / Trailer	1× Camera (front/rear)	RGB, Resolution: 800×600, FOV:90°
	4× Camera (side)	RGB, Resolution: 800×600, FOV:120°
	2× LiDAR	64 channels, 10 Hz capture frequency, 360° horizontal FOV, $-30^\circ$ to $5^\circ$ vertical FOV, 1.536 M points per second, 120 m capturing range
CAV	4× Camera	RGB, Resolution: 800×600, FOV:90°
	1× LiDAR	64 channels, 10 Hz capture frequency, 360° horizontal FOV, $-30^\circ$ to $10^\circ$ vertical FOV, 1.536 M points per second, 120 m capturing range
RSU	1× Camera	RGB, Resolution: 800×600, FOV:120°
	1× LiDAR	64 channels, 10 Hz capture frequency, 360° horizontal FOV, $-30^\circ$ to $5^\circ$ vertical FOV, 1.536 M points per second, 120 m capturing range

Blueprint system. Concurrently, we configured visual properties (customizable colors, materials, and lighting responses) and dynamic parameters (mass distribution, suspension, and powertrain characteristics) to align with real-world truck specifications. The key parameters are documented in Table I. In this paper, we regard tractor and trailer as separate agents considering real-world operational dynamics, where tractors frequently engage with different trailers.

### B. Sensor configurations

Multi-modal data from multiple perspectives form the cornerstone of cooperative perception systems. To ensure comprehensive and reliable data acquisition, each agent (tractor, trailer, CAV, and RSU) is equipped with a carefully designed sensor suite comprising LiDAR, RGB cameras, and IMU units. Table II summarizes the detailed sensor specifications, and Figure 3 illustrates the sensor coordinate system and spatial layout across all platforms.

For CAVs, the baseline configuration includes a roof-mounted LiDAR paired with four strategically positioned RGB cameras providing full 360° coverage. In contrast, the truck's extended physical dimensions (tractor and trailer) necessitate a distributed sensing architecture: two LiDARs are installed at the upper front corners of the tractor, while two additional LiDARs monitor the trailer's rear quadrant. This configuration is complemented by five RGB cameras – two on each lateral side and one at the tractor's front/trailer's rear – ensuring continuous environmental monitoring across the articulated vehicle's entire length. The RSU configuration integrates a LiDAR and a camera oriented toward traffic flow. To optimize coverage and cost-effectiveness, the majority of RSUs in our dataset are deployed on traffic light poles at lane centers or intersection corners. Considering the high pedestrian density in urban scenarios, the LiDAR is mounted at a four-meter height to minimize blind spots in close-range sensing while maintaining practical coverage. This balanced design enhances

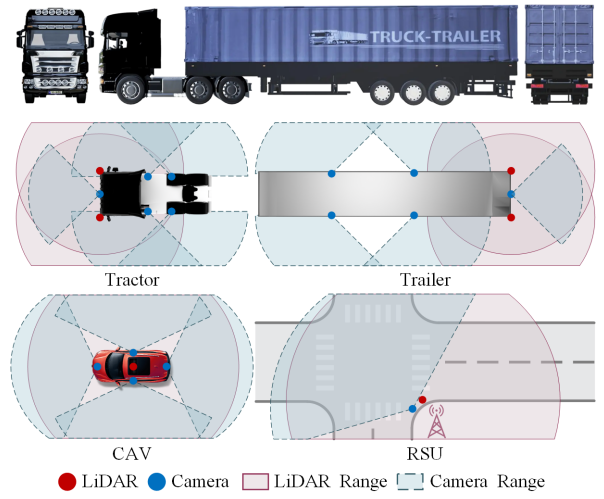


Fig. 3: Illustration of sensor configurations for the agents.

detection reliability at urban intersections where frequent vehicle-pedestrian interactions occur.

### C. Scenarios

The dataset was built using CARLA's simulation platform, which provides an affordable way to recreate complex driving situations with realistic details. CARLA's flexible design allows the creation of different city environments with adjustable sensors, capturing high-quality data that includes precise pixel-level labels. In this system, semi-trucks, intelligent vehicles, and roadside devices work together through vehicle communication technology, forming a connected traffic network. We generated scenarios by adding computer-controlled vehicles and pedestrians randomly appearing at key road locations. These digital traffic elements follow basic traffic rules when moving, but have some controlled randomness in their routes. The primary focus vehicles (semi-trucks and smart cars) are placed in areas with roadside sensors, positioned according to each map's layout and traffic patterns to cover critical urban driving situations. Data collection included different environment types: country roads, busy city streets, highways, and various intersections (four-way, T-shaped, ramps, and roundabouts). The simulation used all available CARLA models, including 35 vehicle types (13 heavy vehicles and 22 light vehicles) plus 19 vulnerable road users (VRUs) types. CARLA's self-driving system and crash prevention features helped create natural traffic movements matching real-world behavior. Some typical scenarios are shown in Figure 4.

### D. Dataset splits

Our dataset follows the format of the OpenCOOD framework [8] for cooperative perception, comprising 64 representative scenarios with diverse vehicle and pedestrian types. Each scenario spans 17-60 seconds and includes multi-modal data from four agents: tractor, trailer, CAV, and RSU, captured from multiple perspectives. Compared to existing datasets, our scenarios demonstrate more complex inter-agent occlusion patterns as illustrated in Figure 4. Sensor data acquisition

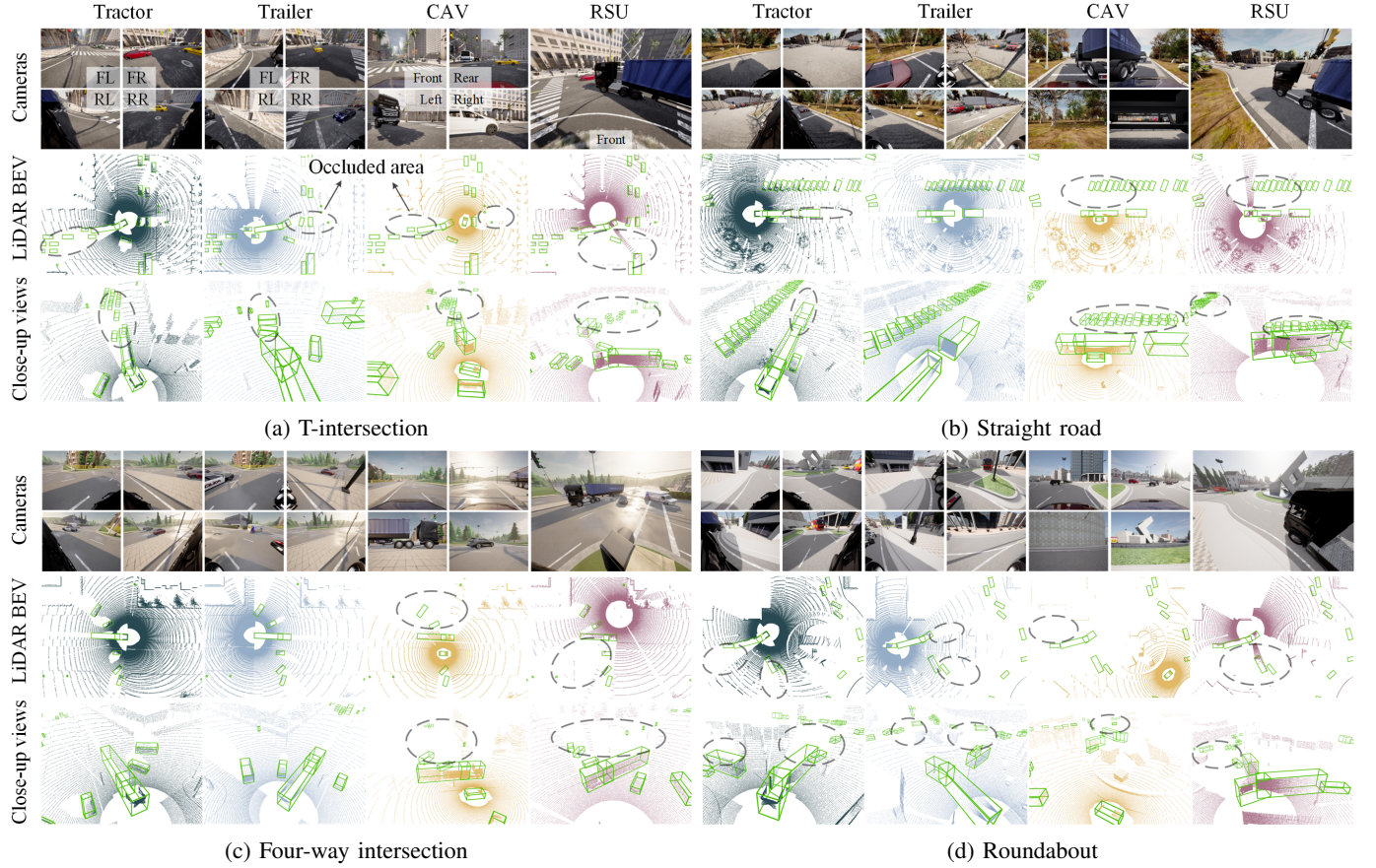


Fig. 4: Four representative scenarios in our dataset: T-intersection, straight road, four-way intersection, and roundabout. In each scenario, the top row shows RGB images from agent perspectives; the middle row displays BEV projections of LiDAR point clouds; the bottom row highlights occluded areas in close-up views, where dashed ellipses annotate critical blind zones for each agent (trailer obstructs tractor and truck obstructs others). All scenarios present the agent sequence from left to right as tractor, trailer, CAV, and RSU.

occurs at 10 Hz, yielding 88,396 synchronized LiDAR-image frames totaling 149.6 GB. The dataset is divided into train, validation, and test sets, with the training set containing 38 scenarios (13,243 frames), the validation set 9 scenarios (2,839 frames), and the testing set 17 scenarios (6,017 frames).

#### E. Data statistics

Figure 5 provides some statistics in the dataset. The scenario duration analysis in Figure 5a reveals an average of 345 frames per scenario, balancing the temporal continuity of cooperative behaviors with data efficiency. Spatial relationships between agents are quantified in Figure 5b, showing that truck-RSU and CAV-RSU distances predominantly remain under 80 meters, while truck-CAV interactions exhibit greater variability with occasional separations exceeding 80 meters. Agent dynamics are further characterized in Figure 5c, where both truck and CAV primarily operate below  $8 \text{ m}\cdot\text{s}^{-1}$ . The CAV demonstrates occasional higher-speed maneuvers, while traffic light waiting phases explain observed low-speed instances. Cooperative perception analysis in Figure 5f indicates the tractor-trailer pair shares the most co-visible objects (average 53 per frame, peaking at 166), followed by truck-RSU and CAV-RSU pairs, with truck-CAV having the least overlap. Articulation patterns

in Figure 5d reveal frequent straight-line motion alongside substantial turning/lane-change maneuvers. Complementing these macroscopic insights, Figure 5e details object category distribution across seven classes, reflecting real-world traffic composition with light vehicles (65%, cars and vans), VRUs (20%, pedestrians, bicyclists, and motorcyclists), and heavy vehicles (15%, truck and buses). Motion analysis in Figure 5h shows most vehicles moving below  $8 \text{ m}\cdot\text{s}^{-1}$  and pedestrian speeds clustering around  $2 \text{ m}\cdot\text{s}^{-1}$ , while stationary vehicles predominantly originate from parking situations and traffic light queues. Proximity analysis in Figure 5g demonstrates pedestrians are more likely than vehicles to appear near agents.

## IV. ANALYSIS OF OCCLUSIONS

### A. Occlusion impacts

TruckV2X captures extensive occlusion scenarios, which are systematically quantified in Figure 6 through object counts across different agent perspectives. On the one hand, the number of occluded objects for the ego truck approximately follows a Gaussian distribution with a mean of 20-30 (Figure 6a). Due to the truck's higher viewpoint, these occlusions primarily originate from static environments like buildings.

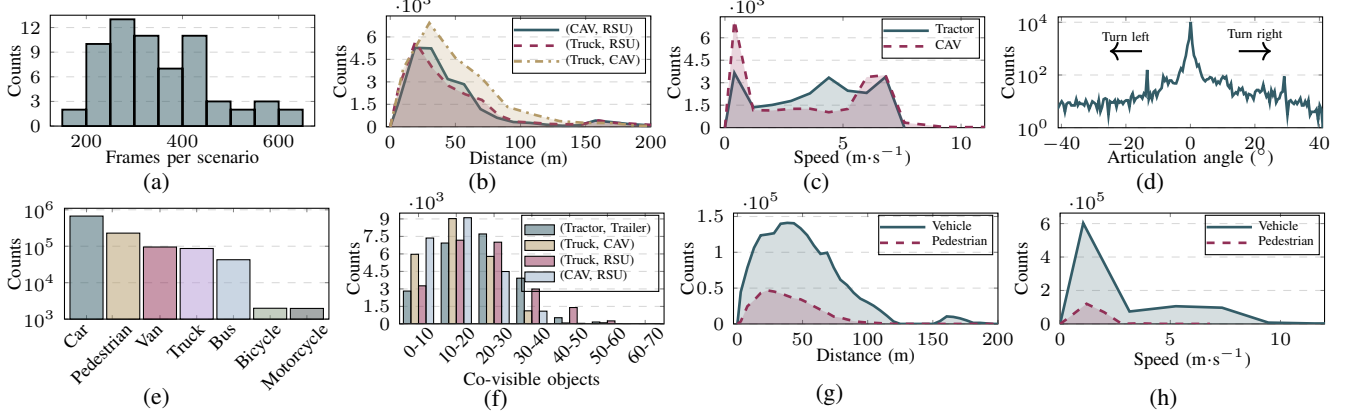


Fig. 5: (a) Frame counts per scenario. (b) Distance statistics between agents. (c) Speed statistics of agents. (d) Articulation angle counts between the tractor and trailer. (e) Object category counts. (f) Statistics of co-visible objects among agents. (g) Distance statistics between objects and agents. (h) Speed statistics of objects.

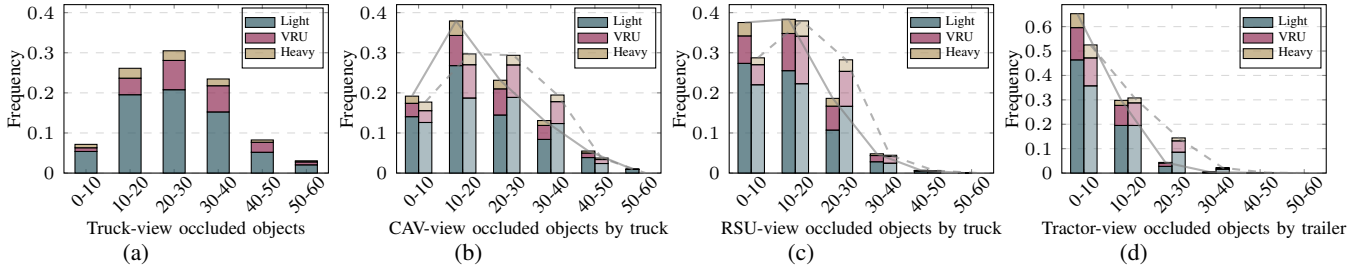


Fig. 6: Distribution of objects occluded for different agents in a 120m range. Distribution of objects occluded (a) from truck; (b) from CAV by truck; (c) from RSU by truck; (d) from the tractor by trailer. Solid lines linking left-side bars denote truck's straight driving scenarios, while dashed lines connecting right-side bars indicate truck's turning scenarios ( $|\text{articulation angle}| > 5^\circ$ ). Light vehicles, heavy vehicles and VRUs are represented by blue, yellow and red colors, respectively.



On the other hand, it reveals that CAVs typically encounter 10-30 objects blocked by truck (Figure 6b), while elevated RSU viewpoints experience less severe impacts, with most cases falling within the 0-20 range (Figure 6c). Notably, trucks exhibit intensified occlusion effects during turning maneuvers, producing measurable increases in obscured object counts. This phenomenon primarily stems from trailers generating localized occlusion patterns that specifically impact their corresponding tractors. While normal driving operations typically result in 0-10 occluded objects, turning conditions demonstrate

obstruction levels rising sharply to 20-30 undetectable targets, as shown in Figure 6d.

### B. Cooperation benefits

Cooperative perception systems mitigate the impacts of occlusion by enabling agents to share perceptual information. To quantify the theoretical upper bound of cooperation benefits, we introduce the occlusion recovery rate, defined as the proportion of an ego agent's occluded objects detected by cooperative ones to its total occluded objects, with values

ranging from 0 to 1. An occlusion recovery rate close to 1 indicates nearly complete blind spot compensation, indicating optimal cooperative perception performance.

Figure 8 illustrates the distribution of occlusion recovery rates for various ego and cooperator configurations. For CAV, the cooperation benefits provided by truck are substantial in most scenarios, with the occlusion recovery rate exceeding 0.8 in over 60% of cases, as shown in Figure 8a. Moreover, most truck-CAV distances are within 50 meters in high occlusion recovery scenarios. As this distance increases, the cooperation benefits deteriorate rapidly. In contrast, the cooperation benefits provided by RSU follow an entirely different trend (Figure 8b). The occlusion recovery rate predominantly falls between 0.4 and 0.6, and RSU is particularly effective in mitigating occlusions at near to mid ranges, whereas truck significantly reduces the occlusions it causes to CAV.

For RSU, the cooperation benefits provided by truck exhibit a trend similar to that of truck benefiting CAV (Figure 8c), with an even higher proportion of cases where the occlusion recovery rate exceeds 0.8. However, the cooperative contribution of CAV to RSU is relatively weak (Figure 8d), with the occlusion recovery rate mostly below 0.4. For truck, RSU provides slightly greater cooperation benefits than CAV, with occlusion recovery rates primarily between 0.4 and 0.6 (Figure 8e), while those from CAV are concentrated between 0.2 and 0.4 (Figure 8f). Additionally, as the distance to truck decreases, the cooperation benefits from both RSU and CAV decline.

Figure 7 illustrates the truck’s occlusion effects through an intersection scenario. The plot shows inverse trends in occlusion recovery rates: truck’s rate decreases over time while RSU’s increases. This occurs because truck initially blocks the CAV’s view when adjacent, making its sensor data crucial for compensating blind zones. As the CAV progresses through the intersection, truck’s influence diminishes while the elevated RSU gradually becomes the dominant perception source.

The above analysis reveals trucks’ dual role as occlusion sources and potential mobile perception platforms, with their dynamic sensing enabling collaborative blind zone reduction for occlusion-resilient autonomous trucking.

## V. BENCHMARK EXPERIMENTS

Following standard practices in truck perception [10] and cooperative perception research [8], [9], we establish object detection benchmarks using mean Average Precision (mAP) with Intersection-over-Union (IoU) thresholds of 0.3, 0.5, and 0.7 for three object categories: heavy vehicles, light vehicles, and VRUs. The evaluation framework incorporates multiple ego agent configurations (as per Figure 8’s cooperative benefit variations) within a detection range of  $x \in [-128, 128]$ m and  $y \in [-64, 64]$ m. Agent communication is constrained to a 300 m to reflect realistic vehicular networking capabilities. Due to significant occlusions in our TruckV2X dataset, we filter out bounding boxes for each agent where the number of LiDAR points within the box is below category-specific thresholds (5 points for VRUs and 15 for vehicles).

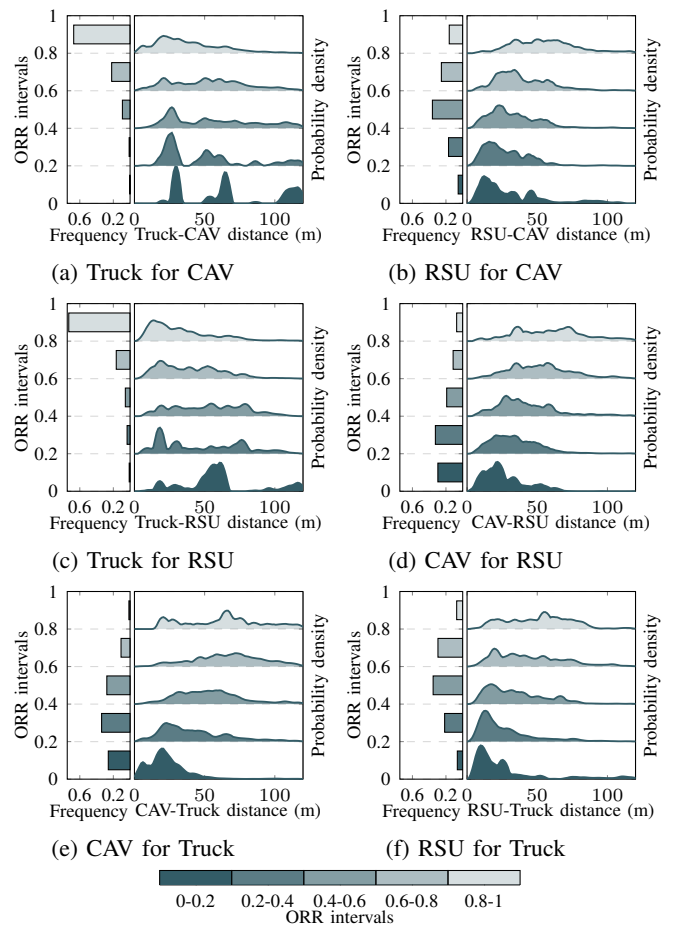


Fig. 8: Frequency distribution of occlusion recovery rates (ORR) across various ego and cooperator configurations, with superimposed probability density distributions of inter-agent distances stratified by ORR intervals.

### A. Experimental setup

To comprehensively test the cooperative perception baselines on TruckV2X, we build several models upon the OpenCOOD framework [8] and perform a comprehensive performance analysis. Specifically, we evaluate three cross-agent fusion strategies: early, intermediate, and late fusion. In early fusion, LiDAR point clouds from collaborating agents are spatially aligned to the ego vehicle’s coordinate system using shared pose data, creating consolidated point cloud inputs for detection models. For intermediate fusion, we implement five state-of-the-art collaborative perception frameworks: F-Cooper [21], V2VNet [22], AttFuse [8], CoBEVT [23], and ERMVP [24]. These methods enable multi-agent collaboration by fusing intermediate feature representations from individual perception models. Late fusion adopts a decentralized paradigm where each agent shares its calibrated pose and confidence-scored detection boxes. The multi-source detections are geometrically projected onto the ego coordinate system and consolidated through standard non-maximum suppression (NMS). All models are trained by 120 epochs with an initial learning rate of 0.001 using the Adam optimizer (weight decay  $\lambda = 10^{-4}$ ). The learning policy combines

TABLE III: Benchmark detection results of SOTA (state-of-the-art) cooperative perception methods on TruckV2X, with truck, CAV, and RSU acting as ego in mutual collaboration, where tractor and trailer are integrated via early fusion to function as a unified agent truck. All values are reported as percentages. Detection accuracy is evaluated using Average Precision (AP) and mean Average Precision (mAP) for light vehicles, heavy vehicles, and VRUs at IoU thresholds of 0.3, 0.5, and 0.7.

Ego	Method	AP <sub>light</sub> @IoU			AP <sub>heavy</sub> @IoU			AP <sub>VRU</sub> @IoU			mAP@IoU		
		0.3	0.5	0.7	0.3	0.5	0.7	0.3	0.5	0.7	0.3	0.5	0.7
Truck (tractor and trailer)	Ego only	51.16	47.43	33.31	55.27	53.99	48.62	10.68	2.91	0.20	39.03	34.78	27.38
	Late Fusion	72.15	68.56	53.27	53.41	52.56	48.02	20.66	6.29	0.46	48.74	42.47	33.92
	Early Fusion	<b>77.22</b>	63.25	49.17	<b>71.50</b>	<b>70.86</b>	<b>67.14</b>	<b>25.75</b>	9.52	0.87	<b>58.16</b>	47.88	39.06
	F-Cooper [21]	67.38	65.90	56.20	65.77	65.61	62.57	18.67	7.45	0.82	50.61	46.65	39.86
	V2VNet [22]	72.89	<u>71.55</u>	<u>63.56</u>	<u>68.90</u>	<u>68.70</u>	64.03	19.74	8.52	0.95	53.84	49.59	<u>42.85</u>
	AttFuse [8]	<u>73.75</u>	<b>72.75</b>	<b>63.74</b>	67.79	67.53	<u>64.79</u>	22.24	<u>10.27</u>	<u>1.16</u>	54.59	<b>50.18</b>	<b>43.23</b>
CAV	CoBEVT [23]	71.93	70.21	60.24	67.82	67.35	63.94	<u>25.53</u>	<b>11.91</b>	<b>1.35</b>	<u>55.09</u>	<u>49.83</u>	41.84
	ERMVP [24]	67.93	66.33	56.53	65.78	65.47	62.50	21.63	9.37	0.94	51.78	47.39	39.99
	Ego only	48.13	46.01	35.99	38.73	34.71	25.61	10.35	3.39	0.28	32.40	28.04	20.63
	Late Fusion	72.73	70.46	58.34	53.44	52.59	48.60	22.86	7.89	0.64	49.68	43.65	35.86
	Early Fusion	<b>79.10</b>	<b>76.97</b>	67.08	<b>71.96</b>	<b>70.89</b>	<b>65.79</b>	<b>29.65</b>	<b>11.68</b>	<b>1.04</b>	<b>60.24</b>	<b>53.18</b>	44.64
	F-Cooper [21]	75.12	73.85	65.01	64.26	63.86	59.25	18.32	6.39	0.50	52.57	47.70	40.92
RSU	V2VNet [22]	75.35	74.28	65.70	67.95	67.54	60.85	18.09	6.37	0.55	53.80	49.40	42.32
	AttFuse [8]	<u>77.54</u>	<u>76.63</u>	<b>69.43</b>	<u>69.91</u>	<u>69.57</u>	64.26	<u>23.05</u>	<u>9.02</u>	<u>0.90</u>	<u>56.83</u>	<u>51.74</u>	<b>44.86</b>
	CoBEVT [23]	74.62	72.98	62.39	64.45	63.77	57.56	20.67	8.56	0.85	53.25	48.44	40.27
	ERMVP [24]	75.47	74.00	64.20	61.97	61.46	55.45	22.66	8.32	0.72	53.36	47.93	39.79
	Ego only	51.54	48.37	35.95	50.45	47.99	41.10	14.72	4.82	0.41	38.90	33.73	25.82
	Late Fusion	<u>73.50</u>	<u>70.60</u>	<u>57.37</u>	49.13	48.18	43.71	19.84	6.16	0.46	47.49	41.65	33.85
RSU	Early Fusion	<b>76.82</b>	<b>73.44</b>	<b>59.77</b>	<b>70.06</b>	<b>68.42</b>	<b>63.51</b>	<b>30.12</b>	<b>11.20</b>	<u>1.04</u>	<b>59.00</b>	<b>51.02</b>	<b>41.44</b>
	F-Cooper [21]	60.75	60.12	53.58	59.77	58.74	53.74	19.77	8.21	0.92	46.76	42.36	36.75
	V2VNet [22]	65.60	64.65	56.07	<u>63.22</u>	<u>62.65</u>	57.71	21.20	8.38	0.82	50.01	45.14	38.53
	AttFuse [8]	64.53	63.62	57.30	62.77	62.39	<u>59.17</u>	<u>26.03</u>	<u>11.17</u>	<b>1.19</b>	<u>51.11</u>	<u>45.73</u>	<u>39.22</u>
	CoBEVT [23]	61.10	60.36	52.87	51.68	51.07	46.26	23.49	10.28	1.02	45.42	40.57	33.38
	ERMVP [24]	63.39	62.50	55.34	56.08	54.50	49.95	20.52	8.24	0.81	46.66	41.75	35.34

TABLE IV: Benchmark detection results of SOTA (state-of-the-art) cooperative perception methods on TruckV2X, with tractor (ego) and trailer collaborating. All values are reported as percentages. Detection accuracy is evaluated using Average Precision (AP) and mean Average Precision (mAP) for light vehicles, heavy vehicles, and VRUs at IoU thresholds of 0.3, 0.5, and 0.7.

Ego	Method	AP <sub>light</sub> @IoU			AP <sub>heavy</sub> @IoU			AP <sub>VRU</sub> @IoU			mAP@IoU		
		0.3	0.5	0.7	0.3	0.5	0.7	0.3	0.5	0.7	0.3	0.5	0.7
Tractor	Ego only	58.80	51.18	32.71	62.63	61.26	56.28	16.93	5.45	0.43	46.12	39.30	29.81
	Late Fusion	<u>71.43</u>	61.83	42.15	<u>65.06</u>	64.02	59.15	24.11	8.32	0.71	53.53	44.72	34.00
	Early Fusion	<b>76.70</b>	63.40	48.00	<b>73.06</b>	<b>72.19</b>	<b>67.66</b>	<b>28.51</b>	<b>11.88</b>	<u>1.19</u>	<b>59.42</b>	<b>49.16</b>	38.95
	F-Cooper [21]	66.45	65.25	55.28	68.89	68.43	63.34	19.97	8.36	0.85	51.77	47.35	39.82
	V2VNet [22]	71.00	<b>69.84</b>	<b>60.72</b>	68.13	67.59	63.75	17.73	7.46	0.77	52.29	48.30	<b>41.75</b>
	AttFuse [8]	65.94	64.91	55.97	<u>69.76</u>	<u>69.28</u>	<u>64.83</u>	<u>22.98</u>	<u>10.16</u>	<b>1.20</b>	<u>52.89</u>	<u>48.12</u>	<u>40.67</u>
Tractor	CoBEVT [23]	66.54	65.07	53.88	63.03	62.61	58.07	19.85	8.70	0.91	49.81	45.46	37.62
	ERMVP [24]	69.56	<u>67.92</u>	<u>57.40</u>	62.90	62.40	59.18	19.36	7.52	0.69	50.61	45.95	39.09

cosine annealing scheduling with 20 warmup epochs. Three standard point cloud augmentations are used: random scaling, rotation, and flipping.

### B. Results and analysis

The results are presented in Table III and IV. For all categories, early fusion integrates point clouds with minimal information loss, resulting in higher AP than other methods. For light vehicles and VRUs, the Average Precision progressively improves from no fusion (ego-only baseline) through late fusion to early fusion configurations, regardless of the selected ego agent. Late fusion achieves substantially higher AP values than the no-fusion baseline, while intermediate fusion exhibits minimal performance variations. In light vehicle detection scenarios, intermediate fusion approaches achieve early fusion performance levels when the CAV serves as the ego agent.

When truck or tractor units assume the ego role, intermediate fusion performance matches late fusion baselines. Notably, RSU-based ego configurations show degraded intermediate fusion performance with over 10% AP reduction compared to late fusion. This can be attributed to increasing discrepancies among CAV, truck, and RSU. Both truck and RSU have viewpoint differences relative to CAV, and RSU is static. As most intermediate fusion methods are CAV-centered, larger discrepancies lead to more pronounced performance degradation. VRU detection displays distinct characteristics, with most intermediate fusion methods marginally surpassing late fusion performance. A subset of these methods even exceeds early fusion results. Heavy vehicle detection reveals contrasting behavior: late fusion underperforms the no-fusion baseline when truck or RSU units act as ego agents. Early fusion consistently outperforms late fusion by over 10% AP across

all configurations, while maintaining narrower performance gaps with intermediate fusion approaches. All methods show minimal VRU detection differences, likely from smaller size and sparser point clouds worsening difficulty. Heavy vehicles' large scale often shows only one side per viewpoint, causing late fusion degradation from low accuracy. Early and intermediate fusion aggregates multi-view info for full contours, boosting accuracy significantly.

Additionally, we observe that as the IoU threshold increases, early fusion AP for light vehicles drops significantly, especially when the ego is a truck or tractor. At an IoU of 0.7, early fusion underperforms all intermediate fusion methods. However, it is not an issue for heavy vehicles, where early fusion consistently achieves the highest AP. This may stem from relative pose errors between the tractor and trailer, causing incomplete point cloud alignment. Light vehicles' smaller size makes their AP more susceptible to such effects than heavy vehicles. Overall, intermediate fusion performs comparably to early fusion when the ego is CAV but is often inferior to late fusion otherwise. This might stem from viewpoint differences between truck, RSU, and CAV. Further research is needed to explore cooperative perception involving truck and RSU, particularly interactions between the tractor and trailer.

## VI. CONCLUSIONS

We present TruckV2X, the first truck-centric cooperative perception dataset capturing complex, occluded scenarios with heavy vehicle interactions. It features synchronized multi-agent observations from tractors, trailers, CAVs, and RSUs, all equipped with comprehensive sensors. Our benchmarks establish baselines for object detection using state-of-the-art cooperative perception methods. Analysis highlights trucks' dual role as both occlusion sources and potential mobile perception platforms, with their dynamic sensing reducing blind spots for resilient autonomous trucking. However, our dataset lacks diverse weather, pedestrian-vehicle hazards, and sensor noise. Beyond blind spots and occlusions, bridging these sim-to-real gaps demands continuous refinement in the real world. We hope this research stimulates new directions in truck-oriented cooperative perception and encourages practical contributions for deployment.

## REFERENCES

- P. Slowik and B. Sharpe, "Automation in the long haul: Challenges and opportunities of autonomous heavy duty trucking in the united states." ICCT Washington, DC, USA, 2018. [1](#)
- T. Ehlgren, T. Pajdla, and D. Ammon, "Eliminating blind spots for assisted driving." *IEEE Transactions on Intelligent Transportation Systems*, vol. 9, no. 4, pp. 657–665, 2008. [1](#)
- M. Ahrholdt, G. Grubb, and E. Agardt, "Intersection safety for heavy goods vehicles," *Advanced Microsystems for Automotive Applications 2009: Smart Systems for Safety, Sustainability, and Comfort*, pp. 87–96, 2009. [1](#)
- Bosch Mobility, "Blind spot detection for heavy commercial vehicles." [Online]. Available: <https://www.bosch-mobility.com/en/solutions/assistance-systems/blind-spot-detection-cv/> [1](#), [2](#)
- ZF Group, "Onside blind spot detection system." [Online]. Available: [https://www.zf.com/products/en/cv/products\\_64618.html](https://www.zf.com/products/en/cv/products_64618.html) [1](#), [2](#)
- H. Caesar, V. Bankiti, A. H. Lang, S. Vora, V. E. Liou, Q. Xu, A. Krishnan, Y. Pan, G. Baldan, and O. Beijbom, "nuscenes: A multimodal dataset for autonomous driving," in *Proceedings of the IEEE/CVF conference on computer vision and pattern recognition*, 2020, pp. 11 621–11 631. [2](#)
- P. Sun, H. Kretzschmar, X. Dotiwalla, A. Chouard, V. Patnaik, P. Tsui, J. Guo, Y. Zhou, Y. Chai, B. Caine *et al.*, "Scalability in perception for autonomous driving: Waymo open dataset," in *Proceedings of the IEEE/CVF conference on computer vision and pattern recognition*, 2020, pp. 2446–2454. [2](#)
- R. Xu, H. Xiang, X. Xia, X. Han, J. Li, and J. Ma, "Opv2v: An open benchmark dataset and fusion pipeline for perception with vehicle-to-vehicle communication," in *2022 International Conference on Robotics and Automation (ICRA)*. IEEE, 2022, pp. 2583–2589. [2](#), [3](#), [6](#), [7](#)
- H. Yu, Y. Luo, M. Shu, Y. Huo, Z. Yang, Y. Shi, Z. Guo, H. Li, X. Hu, J. Yuan *et al.*, "DAIR-V2X: A large-scale dataset for vehicle-infrastructure cooperative 3d object detection," in *Proceedings of the IEEE/CVF Conference on Computer Vision and Pattern Recognition*, 2022, pp. 21 361–21 370. [2](#), [6](#)
- F. S. Fent, F. Kuttnerreich, F. Ruch, F. Rizwin, S. Juergens, L. Lechermann, C. Nissler, A. Perl, U. Voll, M. Yan *et al.*, "MAN TruckScenes: A multimodal dataset for autonomous trucking in diverse conditions," in *The Thirty-eight Conference on Neural Information Processing Systems Datasets and Benchmarks Track*, 2024. [2](#), [6](#)
- A. Dosovitskiy, G. Ros, F. Codevilla, A. Lopez, and V. Koltun, "Carla: An open urban driving simulator," in *Conference on robot learning*. PMLR, 2017, pp. 1–16. [2](#)
- Z. Dong, M. Fu, H. Liang, C. Zhu, and Y. Yang, "DSVT: Dynamic 3d surround view for tractor-trailer vehicles based on real-time pose estimation with drop model," in *2024 IEEE/RSJ International Conference on Intelligent Robots and Systems (IROS)*. IEEE, 2024, pp. 9461–9467. [2](#)
- S. Yoo, H. S. Lee, H. Myeong, S. Yun, H. Park, J. Cho, and D. H. Kim, "End-to-end lane marker detection via row-wise classification," in *Proceedings of the IEEE/CVF conference on computer vision and pattern recognition workshops*, 2020, pp. 1006–1007. [2](#)
- H. Xiang, Z. Zheng, X. Xia, R. Xu, L. Gao, Z. Zhou, X. Han, X. Ji, M. Li, Z. Meng *et al.*, "V2x-real: a largs-scale dataset for vehicle-to-everything cooperative perception," in *European Conference on Computer Vision*. Springer, 2024, pp. 455–470. [2](#)
- A. Geiger, P. Lenz, C. Stiller, and R. Urtasun, "Vision meets robotics: The kitti dataset," *The International Journal of Robotics Research*, vol. 32, no. 11, pp. 1231–1237, 2013. [2](#)
- C. Shooter and J. Reeve, "Intersafe-2 architecture and specification," in *2009 IEEE 5th International Conference on Intelligent Computer Communication and Processing*. IEEE, 2009, pp. 379–386. [2](#)
- F.-E. Braiteh, F. Bassi, and R. Khatoun, "Platooning in connected vehicles: A review of current solutions, standardization activities, cybersecurity, and research opportunities," *IEEE Transactions on Intelligent Vehicles*, 2024. [2](#)
- Z. Song, L. Yang, F. Wen, and J. Li, "Traf-align: Trajectory-aware feature alignment for asynchronous multi-agent perception," in *Proceedings of the Computer Vision and Pattern Recognition Conference*, 2025, pp. 12 048–12 057. [2](#)
- W. Zimmer, G. A. Wardana, S. Sritharan, X. Zhou, R. Song, and A. C. Knoll, "Tumtraf V2X cooperative perception dataset," in *Proceedings of the IEEE/CVF Conference on Computer Vision and Pattern Recognition*, 2024, pp. 22 668–22 677. [2](#)
- L. Yang, X. Zhang, J. Li, C. Wang, Z. Song, T. Zhao, Z. Song, L. Wang, M. Zhou, Y. Shen *et al.*, "V2X-Radar: A multi-modal dataset with 4D radar for cooperative perception," *arXiv preprint arXiv:2411.10962*, 2024. [2](#)
- Q. Chen, X. Ma, S. Tang, J. Guo, Q. Yang, and S. Fu, "F-cooper: Feature based cooperative perception for autonomous vehicle edge computing system using 3d point clouds," in *Proceedings of the 4th ACM/IEEE Symposium on Edge Computing*, 2019, pp. 88–100. [6](#), [7](#)
- T.-H. Wang, S. Manivasagam, M. Liang, B. Yang, W. Zeng, and R. Urtasun, "V2vnet: Vehicle-to-vehicle communication for joint perception and prediction," in *Computer Vision–ECCV 2020: 16th European Conference, Glasgow, UK, August 23–28, 2020, Proceedings, Part II 16*. Springer, 2020, pp. 605–621. [6](#), [7](#)
- R. Xu, Z. Tu, H. Xiang, W. Shao, B. Zhou, and J. Ma, "Cobevt: Cooperative bird's eye view semantic segmentation with sparse transformers," *arXiv preprint arXiv:2207.02202*, 2022. [6](#), [7](#)
- J. Zhang, K. Yang, Y. Wang, H. Wang, P. Sun, and L. Song, "Ermvp: Communication-efficient and collaboration-robust multi-vehicle perception in challenging environments," in *Proceedings of the IEEE/CVF Conference on Computer Vision and Pattern Recognition*, 2024, pp. 12 575–12 584. [6](#), [7](#)